Numerical simulation of OH* chemiluminescence in acoustically forced planar premixed flames

C. Jiménez
CIEMAT, Avenida Complutense, 22, 28040, Madrid, Spain
H. Schmidt
BTU Cottbus, Siemens-Halske-Ring 14, D-03046 Cottbus, Germany

Abstract

In this work we present numerical simulations of the response of a planar premixed methane flame to acoustic perturbations. We extend our previous work [1] and add chemical mechanisms to account for OH* formation and de-excitation via collisional quenching and light emission. The obtained oscillating response of the heat release rate and the OH* chemiluminescence emission rate are compared to the experimental measurements of chemiluminescence of OH* of Wangher et al. [2, 3]. Our simulations predict an important phase shift between the OH* light signal and the forcing pressure for low frequencies, very close to what was found in the experiments. This high phase shift, which is not observed in the heat release rate response, shows that the OH* signal is not always correlated to the heat release signal.

1 Introduction

Chemiluminescence of excited radicals is a widely used diagnosis tool for combustion studies. The detection of the naturally emitted light from excited radicals has been used to identify the reaction zone, as a measure of the equivalence ratio or to estimate the heat release rate [4, 5, 6, 7, 8]. Still, there is some evidence that the relation between the measured chemiluminescence and heat release could be pressure dependent [6, 7], and could also change locally with curvature and strain rate in unsteady flames [9, 10, 11]. These results cast some doubt about the assumption of proportionality between the heat release rate and the chemiluminescence intensity under general conditions, in which other parameters can vary along the measured flames.

A key issue for the design of enclosed combustion devices, e.g., low-emission gas turbines, industrial boilers, and household burners is that fluctuating heat release may interact with resonant modes of the combustion chamber leading to very high pressure oscillations [12, 13]. In Wangher et al. [2] and Wangher's Ph.D. thesis [3] the first attempt to measure the direct effect of acoustic pressure fluctuations in a flame was undertaken. They measured the chemiluminescence of the radical OH* in a lean planar premixed

methane flame, excited by low amplitude acoustic waves of frequencies close to the characteristic flame time. Assuming that the OH* measured signal was proportional to heat release, they compared the OH* oscillations' amplitude and phase to the analytical model of flame response proposed by Clavin et al. [14], based on one–step Arrhenius kinetics. The amplitude of the OH* signal could be related to the predictions of that model. An even closer agreement was found with a higher complexity flame response model, including a two-step chemical mechanism, proposed by Clavin and Searby [15]. But the measurements showed a phase shift between the OH* measured signal and the pressure signal of up to $\pi/2$ for low frequencies, a shift that none of the models could predict. Wangher [3] gives two possible explanations, (i) it could be that more complex models, including more detailed chemistry with further radicals are needed to be able to reproduce the behavior of the flame in experiments, or (ii) it could be that OH* chemiluminescence intensity, the magnitude measured in experiments, is not directly proportional to the heat release rate, the quantity modeled in the mentioned analytical studies.

In [1] we used numerical simulations with detailed thermodynamics, transport and chemical kinetics to study the response of a planar premixed methane flame to acoustic perturbations. Here we extend our previous work and add chemical mechanisms to account for OH* formation and de-excitation via collisional quenching and light emission. We use two different codes and two different OH* mechanisms to verify our results. In our simulations we measure the response of the heat release and the OH* chemiluminescence to pressure oscillations, and compare both results to the experimental measurements of chemiluminescence of OH* of Wangher et al. [2]. We will show that the heat release oscillations and the OH* chemiluminescence oscillations are not necessarily in phase.

2 Numerical set up

We use numerical experiments to investigate 1-D premixed flames interacting with acoustic waves of characteristic times of similar order and with wavelength much longer than the flame width, as presented in Fig. 1.

A planar premixed steady methane/air flame with $\phi = 0.625$, 300 K inflow temperature and a pressure of 1 atm, corresponding to a flame speed s_L of about 15 cm/s and a flame width $\delta_f = 1$ mm is first established. We use 1000 grid points on a 7 mm domain[1]. Acoustic waves are then imposed

[1]Some compressible calculations, corresponding to the smallest frequencies, needed a

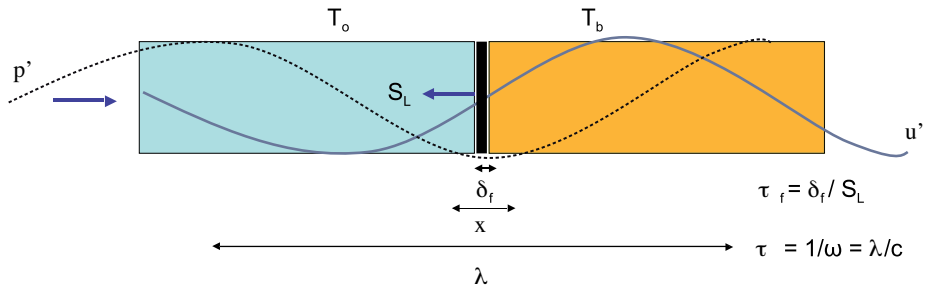

Figure 1: Sketch of the studied problem

with an amplitude $p' = 500$ Pa and frequencies ω ranging from 1 Hz to 5000 Hz, corresponding to reduced frequencies $\omega\tau_f$=.0067 to 33.33, where $\tau_f = \delta_f/s_L = 1/150$ is the flame transit time.

We are interested in the effect of waves of small amplitude p' and moderate frequency, that is, with ω of the order of the inverse of the flame transit time, still in the linear regime studied by Clavin et al. [14] or McIntosh [16, 17]. The characteristic times associated to the wave and the flame are $\tau = 1/\omega = \lambda/c$ and $\tau_f = \delta_f/s_L$, respectively, and the flame Mach number, $Ma = s_L/c$ is much smaller than one. This corresponds to $\omega\tau_f = \tau_f/\tau = O(1)$, and thus to wavelengths much longer than the flame thickness: $\frac{\delta_f/s_L}{\lambda/c} = O(1) \Rightarrow \lambda = \delta_f/Ma >> \delta_f$. Thus in the studied problem acoustic waves are seen by the flame as pulses of time–varying pressure, uniform across the flame width, and no spatial pressure variations can be seen by the flame.

Two different numerical methods are used to double check our results. The first one is an incompressible zero-Mach-number solver, which uses implicit finite differencing, and for which the pressure waves are represented by time fluctuations of the background pressure $p(t)$, see e.g. [18, 19]. While the pressure is changing in time, the flame location is kept constant, which is very close to the experimental setup in [2]. Thermodynamic and transport properties as well as reaction rates are calculated using the C++ interface of the CANTERA software package [20]. The second is a compressible finite difference solver normally used for direct numerical simulations (DNS) and in which the full acoustics are resolved [21]. We use the inlet wave modulation method (IWM [22]), based on NSCBC [23, 21] to impose acoustic

longer domain to capture the flame position fluctuation: 14 mm over 2000 points

waves at the inlet. The solver was designed for DNS of reacting turbulent flows and contains routine to include detailed chemical kinetics and multi species thermodynamic and transport properties.

Diffusion velocities are calculated using a mixture-based formulation with variable Lewis numbers for all species. Further details on the numerical models and previous results of similar simulations, illustrating the equivalence of the two numerical methods in this configuration, can be found in [1].

3 Mechanisms for OH* chemistry

We use the well established GRI3.0 mechanism [24], containing 53 species and 325 reactions, designed to model natural gas combustion and extensively validated. In order to study the correlation between OH* chemilumniscence and heat release, we add a description of the formation of the excited radical OH* and its de-excitation into OH, by collision with other molecules (quenching) and by spontaneous light emission (chemiluminescence).

A review on the mechanisms proposed to account for OH* chemistry (see for instance [11]) shows that most authors agree on the de-excitation reactions and their rates, differing only in the formation reactions or their associated reaction rate coefficients. In this work, we combined GRI3.0 with the mechanism proposed by Hall and Petersen [25], with reactions and parameters as presented in Table 1, and with the mechanism proposed by Kathrotia et al. [26], with reactions and parameters as presented in Table 2. The two mechanisms differ only in the OH* formation paths, and will be shown to give virtually identical results for the OH* de-excitation by chemiluminescence. We name the resulting chemical schemes GRIH and GRIK, respectively. In both cases we used the thermodynamical and transport properties of OH for the radical OH*, except for the formation enthalpy, which we make equal to the formation enthalpy of a molecule of OH, plus the energy of a photon with wavelength $\lambda = 307$ nm ($h^0_{OH*} - h^0_{OH} = 93.5$ kcal/mol).

4 Results

Several simulations of a methane/air planar premixed flame oscillating under acoustic waves of amplitude $500Pa$ and reduced frequencies $\omega\tau_f$ ranging from 0.33 to 30 were conducted. A visualization of the oscillating flame response for two of the simulations, corresponding to selected forcing re-

Reaction	A	n	E_a
$CH+O_2 \rightleftharpoons CO+OH^*$	3.24E14	-0.4	4150.0
$H+O+M \rightleftharpoons OH^*+M$	3.10E14	0.0	10000.0
$OH^*+H2O \rightleftharpoons OH^*+H2O$	5.92E12	0.5	-861.0
$OH^*+H2 \rightleftharpoons OH+H2$	2.95E12	0.5	-444.0
$OH^*+H \rightleftharpoons OH+H$	1.50E12	0.5	0.0
$OH^*+O_2 \rightleftharpoons OH+O_2$	2.10E12	0.5	-482.0
$OH^*+O \rightleftharpoons OH+O$	1.50E12	0.5	0.0
$OH^*+OH \rightleftharpoons OH+OH$	1.50E12	0.5	0.0
$OH^*+CO_2 \rightleftharpoons OH+CO_2$	2.75E12	0.5	-968.
$OH^*+CO \rightleftharpoons OH+CO$	3.23E12	0.5	-787.
$OH^*+CH_4 \rightleftharpoons OH+CH_4$	3.36E12	0.5	-635.
$OH^*+N_2 \rightleftharpoons OH+N_2$	1.08E11	0.5	-1238.0
$OH^* \rightarrow OH$	1.4E6	0.0	0.0

Table 1: Scheme for OH* proposed by Hall and Petersen [25], representing reaction rate coefficients $AT^n exp(-E_a/RT)$ in units of mol, cm, s, cal, K
.

Reaction	A	n	E_a
$CH+O_2 \rightleftharpoons CO+OH^*$	3.24E14	-0.4	4063.0
$H+O+M \rightleftharpoons OH^*+M$	1.20E13	0.0	6931.0
$HCO+O \rightleftharpoons OH^*+CO$	2.89E+11	0.0	461.28
$OH^*+H2O \rightleftharpoons OH+H2O$	5.93E12	0.5	-860.42
$OH^*+H2 \rightleftharpoons OH+H2$	2.95E12	0.5	-454.11
$OH^*+H \rightleftharpoons OH+H$	1.31E13	0.5	-167.30
$OH^*+O_2 \rightleftharpoons OH+O_2$	2.10E12	0.5	-478.01
$OH^*+CO_2 \rightleftharpoons OH+CO_2$	2.76E12	0.5	-979.92
$OH^*+OH \rightleftharpoons OH+OH$	6.01E12	0.5	-764.81
$OH^*+CO \rightleftharpoons OH+CO$	3.23E12	0.5	-788.71
$OH^*+CH_4 \rightleftharpoons OH+CH_4$	3.36E12	0.5	-645.31
$OH^*+N_2 \rightleftharpoons OH+N_2$	1.08E11	0.5	-1242.83
$OH^* \rightarrow OH$	1.45E6	0.0	0.0

Table 2: Scheme for OH* proposed by Kathrotia et al. [26], representing reaction rate coefficients $AT^n exp(-E_a/RT)$ in units of mol, cm, s, cal, K
.

duced frequencies 0.33 and 3.33 is presented in Figure 2. In that figure the total (spatially integrated) heat release rate and the total (spatially integrated) OH* chemiluminescence emission rate oscillations are plotted. Also included are the pressure fluctuations at the domain inlet (equivalent to the pressure fluctuations at the flame position, as the pressure is constant in the computational domain). The plots correspond to results of incompressible simulations using the GRIH mechanism and the GRIK mechanism.

The first evidence is that the two chemical mechanisms give identical results for OH* chemiluminescence: both the amplitude and the phase of the OH* luminiscence intensity are identical in the two sets of results. It also becomes obvious that the heat release signal and the OH* luminescence signal are *not* always correlated:

- The amplitudes of the two response signals are not proportional: the heat release rate oscillations' amplitude is in the two cases bigger than the amplitude of the forcing acoustic waves, while the OH* chemiluminescence signal amplitude becomes smaller for the wave with $\omega\tau = 0.33$.
- For acoustic waves of reduced frequency 3.33, the heat release rate and the chemiluminescence response signals are in phase and slightly advanced with respect to the forcing pressure signal pressure.
- For acoustic waves of reduced frequency 0.33, the OH* chemiluminescence signal is well in advance of the pressure forcing, resulting in a phase shift of about 0.4π.

This behaviour can be observed for the full range of forcing frequencies: In Figures 3 and 4 we plotted the amplitude gain and phase shift corresponding to the total heat release rate and the total OH* chemiluminescence emission rate for forcing frequencies range from 0.33 to 30. The amplitude gain and phase shift are extracted from the spatially integrated heat release (or OH* chemiluminescence reaction rate) signals $\dot{Q}'$ or light intensity I' and are normalized with respect to the mean values $\overline{\dot{Q}}$ and $\overline{I}$ and then also with the amplitude of pressure fluctuations measured with ρc^2 and multiplied by the factor $\frac{RT^b}{Ea(\gamma-1)}$, to reproduce the normalization in [2]. Also included in the plot are the experimental measurements of [2] and the model for $\dot{Q}'/\overline{\dot{Q}}$ as given in [14]. To produce the curves corresponding to the model we used typical values of $\beta = 9$ and 10, $Le = 1$, and $T_b = 1710$ K, characteristic for our flames.

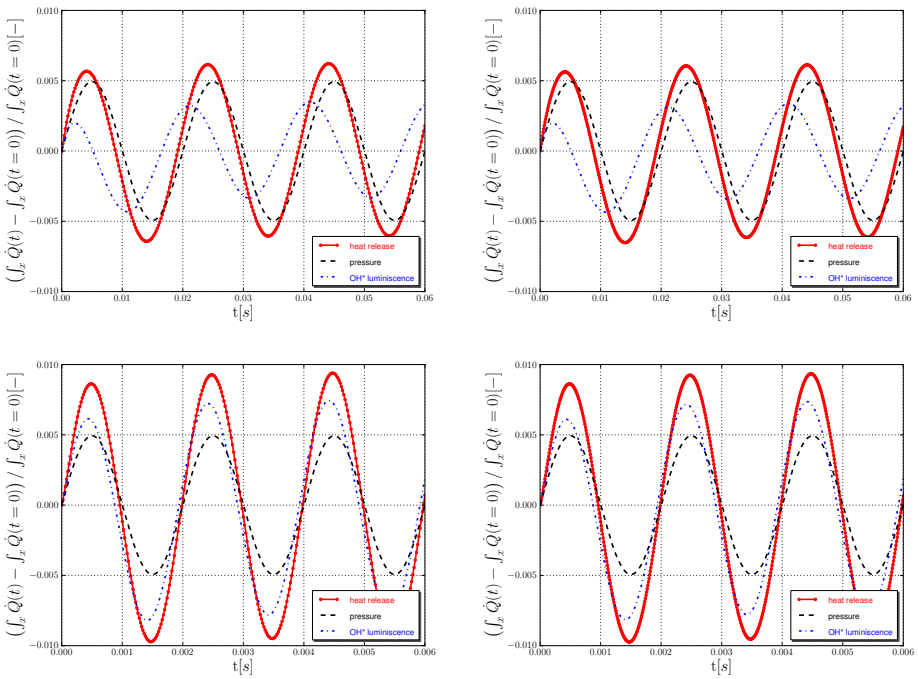

Figure 2: Integrated heat release rate and OH* chemiluminescence intensity oscillations compared to the forcing pressure for acoustic waves of amplitude 500 Pa and reduced frequencies $\omega\tau_f$ 0.33 (top) and 3.33 (bottom). Results correspond to simulations with the incompressible method and the GRIH (left) and GRIK (right) chemical mechanisms.

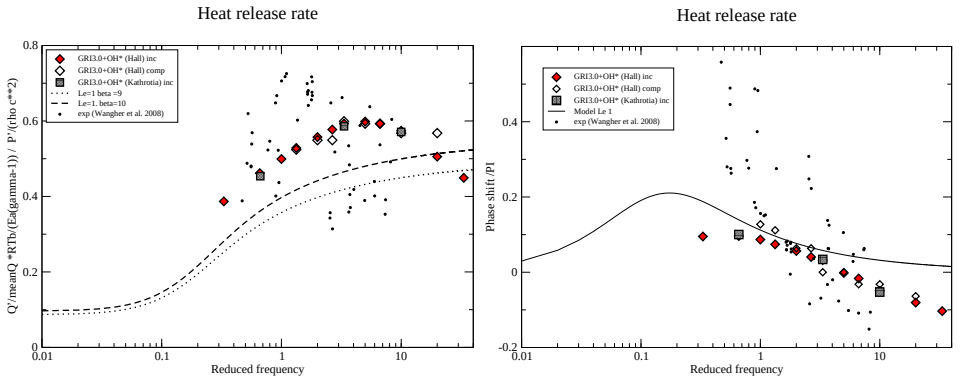

Figure 3: Amplitude gain (left) and phase shift (right) for the integral heat release rate oscillations compared to the forcing acoustic waves pressure

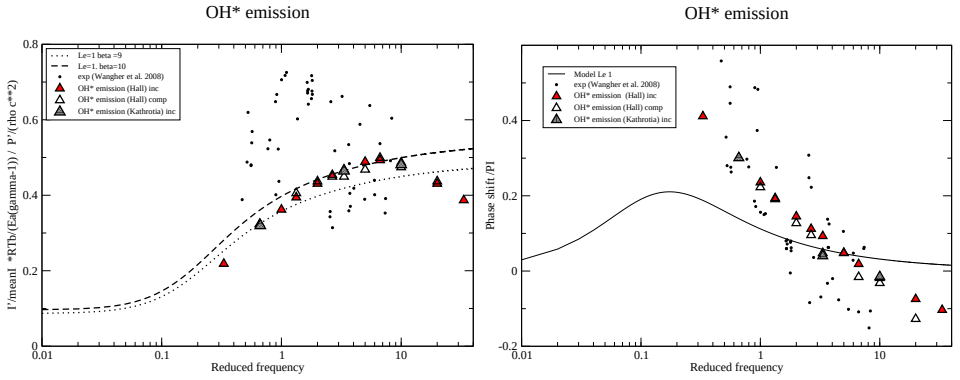

Figure 4: Amplitude gain (left) and phase shift (right) for the integral OH* emission oscillations compared to the acoustic waves pressure

For the full range of simulations the amplitude gain and the phase shift from the forcing pressure signal are similar for incompressible and compressible simulations, as well as for the two chemical mechanisms, GRIH and GRIK (note that only some results for this last mechanism are included, for the sake of clarity). When we compare them with the experimental results, we observe again that:

- The amplitude gain for the heat release rate in Fig. 3 has a magnitude comparable to the experimental measurements and a frequency dependence similar to what the model predicts, but at a slightly higher level. The amplitude gain of the OH* chemiluminescence emission rate $I'/\overline{I}$ is smaller than the amplitude gain of heat release for the full range of frequencies, but still in the range of the experimental results.

- The computed phase shift for the heat release rate signal is frequency dependent and changes from positive to negative at a reduced frequency of about 4, similarly to the experimental measurements. In the low frequency range, however, experiments show a large positive phase shift, growing when the frequency decreases and reaching values of up to $\pi/2$, whilst the numerical simulation results feature a positive but rather constant and small phase shift.

- The computed phase shift for the OH* signal clearly follows the tendency of the experiments: A negative shift, corresponding to a delay of the OH* signal, is obtained for reduced frequencies higher than 8. An large positive shift, that is, an advanced signal,of up tu 0.4π is obtained for the smaller frequency range, in agreement with the experiments.

The numerical simulations allow to reach the low frequency limit, not attainable in the experiments in [2]. We present in figure 5 results corresponding to the first cycle in an additional numerical simulation near the zero frequency limit, namely for a frequency of 1 Hz (or $\omega\tau_f = 0.006$). It is clear that in this simulation the heat release response signal is in phase or slightly in advance with respect to the pressure signal (phase shift about $\pi/50$), while the OH* chemiluminescence signal is in opposition of phase with respect to the pressure signal (phase shift π) . Note that this phase opposition between the OH* luminescence response and the forcing pressure signal in the near-zero frequency limit agrees with results obtained in experiments [6, 7] and simulations [3] on premixed flames subject to quasy steady pressure variations. In those conditions, it was also found that while the total heat release rate increased with pressure, the integrated OH* chemiluminescence intensity decreased with increasing pressure.

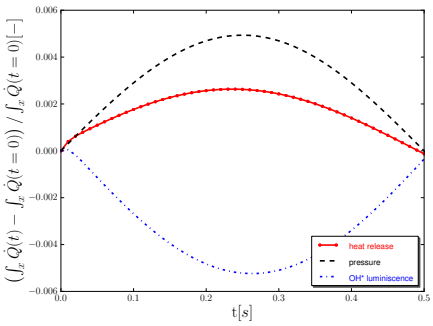

Figure 5: Integrated heat release rate and OH* chemiluminescence intensity compared to the forcing pressure for acoustic waves of amplitude 500 Pa and reduced frequencies $\omega\tau_f$ 0.0067 (1 Hz). Results correspond to simulations with the incompressible method and the GRIH chemical scheme.

It seems clear from these results that the OH* chemiluminescence response to pressure oscillation, what is measured in experiments, is a not necessarily correlated to the heat release response.

5 Conclusions

We present numerical simulations of the OH* chemiluminescence response of a lean methane/air flame to acoustic waves for frequencies of the order of the flame transit time. Two different numerical formulations, one incompressible, one compressible, and two different chemical models, where the models for OH* formation and de-excitation proposed in [25] and in [26] were added to the GRI3.0 mechanism, are used.

The results show that the heat release response and the OH* chemiluminescence response are not necessarily correlated. We show that in our configuration the amplitude gain is of the same order for heat release and OH* emissions, but not exactly proportional. Moreover, we observe that there is an important phase shift between the two response signals for the lower forcing frequencies. The numerical simulations allow to reach the low frequency limit, not attainable in experiments, where we found that the two signals are in phase opposition. These results suggest that OH* chemiluminescence, the quantity measured in experiments, is in general not directly proportional to heat release.

Acknowledgements

This work was partially supported by the Spanish Ministry of Science through project ENE-2008-06515-C04-02 and the Comunidad de Madrid via project S2009/ENE-1597. The authors acknowledge discussions with G. Searby, P. Clavin, J. Quinard and A. Wangher, who also gently provided their experimental data.

References

[1] H. Schmidt, C. Jiménez, Combust. Flame In press.

[2] A. Wangher, G. Searby, J. Quinard, Combust. Flame 154 (2008) 310–318.

[3] A. Wangher, University of Aix–Marseille, Ph.D. thesis (2009).

[4] J. Kojima, Y. Ikeda, T. Nakajima, Proc. Combust. Inst. 28 (2000) 1757–1764.

[5] J. Lee, D. A. Santavicca, J. Propul. Power 19 (5) (2003) 735–750.

[6] N. Docquier, S. Belhalfaoui, F. Lacas, N. Darabiha, C. Rolon, Proc. Combust. Inst. 28 (2000) 1765–1774.

[7] B. Higgins, M. Q. McQuay, F. Lacas, J. C. Rolon, N. Darabiha, S. Candel, Fuel 80 (1) (2001) 67–74.

[8] Y. Hardalupas, M. Orain, Combust. Flame 139 (3) (2004) 188–207.

[9] H. N. Najm, P. H. Paul, C. J. Mueller, P. S. Wyckoff, Combust. Flame 113 (3) (1998) 312–332.

[10] B. Ayoola, R. Balachandran, J. Frank, E. Mastorakos, C. Kaminski, Combust. Flame 144 (1-2) (2006) 1–16.

[11] C. Panoutsos, Y. Hardalupas, A. Taylor, Combust. Flame 156 (2) (2009) 273–291.

[12] S. Candel, Proc. Combust. Inst. 29 (2002) 1–28.

[13] X. Wu, M. Wang, P. Moin, N. Peters, J. Fluid Mech. 497 (2003) 23–53.

[14] P. Clavin, P. Pelcé, L. He, J. Fluid Mech. 216 (1990) 299–322.

[15] P. Clavin, G. Searby, Combust. Theor. Model. 12 (2008) 545–567.

[16] A. C. McIntosh, Combust. Sci. Technol. 91 (1993) 329–346.

[17] A. C. McIntosh, Phil. Trans. R. Soc. A357 (1999) 3523–3538.

[18] R. Klein, J. Comp. Phys. 121 (1995) 213–237.

[19] M. Oevermann, H. Schmidt, A. R. Kerstein, Combust. Flame 155 (2008) 370–379.

[20] D. Godwin, http://www.cantera.org.

[21] M. Baum, T. Poinsot, D. Thévenin, J. Comp. Phys. 116 (1994) 247–261.

[22] A. Kaufmann, F. Nicoud, T. Poinsot, Combust. Flame 13 (2002) 371–385.

[23] T. Poinsot, S. Lele, J. Comp. Phys. 101 (1992) 104–129.

[24] G. P. Smith, D. M. Golden, M. Frenklach, N. W. Moriarty, B. Eiteneer, M. Goldenberg, C. T. Bowman, R. K. Hanson, S. Song, W. C. Gardiner, V. V. Lissianski, Z. Qin, http://www.me.berkeley.edu/gri mech/, Tech. rep.

[25] J. Hall, E. Petersen, Int. J. Chem. Kin. 38 (2006) 714–724.

[26] T. Kathrotia, U. Riedel, J. Warnatz, in: Proc. Eur. Combust. Meet., 2009.